A mathematical model for a partial paratransgenesis system within *L. longipalpis*

iGEM UNILA 2021

(SynFronteras Team)

2021

I. Growth Model

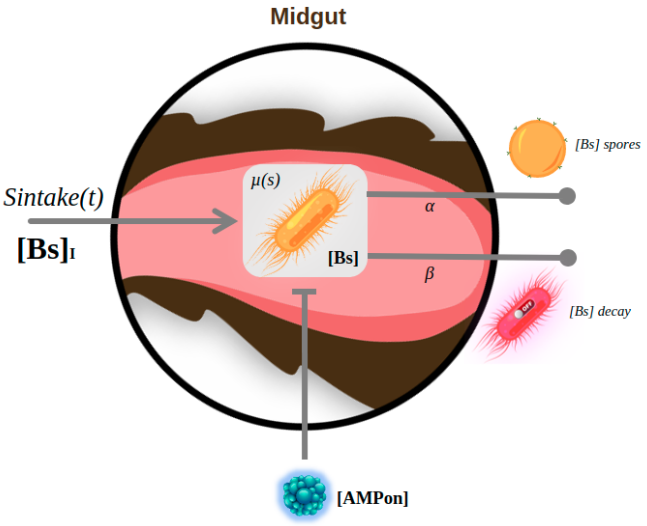

Figure 1: Visual representation of the parameters and functions involved in the growth model.

In the growth model, we assume the complete differentiation from the chassis to the vegetative form. Thus, we calculate the chassis growth rate as a function of substrate availability, probability of re-sporulation, decay rate due to adverse conditions, and [AMP_{on}] toxicity for the chassis (Figure 1).

i) Chassis Growth

$$\frac{d[Bs]}{dt} = V_{Bs,growth} - V_{Bs,death}$$

In our model, *Bacillus subtilis* concentration in the sandfly's midgut depends on growth rate ($\mu(s)$), described by Monod's equation; decay rate (β), represents the constant mortality rate in varying conditions in the midgut; and re-sporulation probability rate (α), a time-dependent parameter that describes the probability of forming a spore at time *t*.

$$V_{Bs,growth} = \mu(s) \times [Bs]$$

$$V_{Bs,death} = \left(\frac{AMP_{on}^{\eta}}{K_{0.5Bs}^{\eta} + AMP_{on}^{\eta}} + \beta + \alpha(t)\right) \times [Bs]$$

$\mu(s)$: *B. subtilis* growth rate (h^{-1});

β: *B. subtilis* decay rate (h^{-1});

$\alpha(t)$: *B. subtilis* sporulation probability rate (h^{-1});

$[Bs]$: *B. subtilis* concentration in the midgut (µg/L);

$K_{0.5Bs}$: IC50 for B. subtilis (nM);

Monod's equation aims to relate bacterial growth rates ($\mu(s)$) to the concentration of substrate-limited $[S]$, where $\mu(s)$ is the specific growth rate for both the nutrient-rich and deficient cases.

$$\mu(s) = \frac{\mu_{max} \cdot [S]}{Ks + [S]} \textit{ (Monod Equation)}$$

$\mu(s)$: *B. subtilis* growth rate (h^{-1});

μ_{max}: maximal growth rate (h^{-1})

S: substrate concentration (µg/L)

The sporulation probability rate (α) is time-dependent which is given by a Gaussian probability density. This equation was described and tested previously[1], the normal distribution is composed of three parameters: α_{max}, the maximal proportion of vegetative cells that can sporulate in a given period of time; t_{max}, the time at which this maximal probability to sporulate is reached; σ, the probability scattering which has an impact on the speed of appearance of spores over time. This sentence describes the probability of the chassis returning to its sporulated form.

$$\alpha(t_i) = \alpha_{max} \frac{1}{\sqrt{2\pi}\cdot\sigma} exp\left[-0.5\left(\frac{t_i - t_{max}}{\sigma\sqrt{2}}\right)^2 \right] \text{ (Gaussian function)}$$

α_{max}: Maximal proportion of sporulating vegetative cells;

t_{max}: Time at maximal probability to sporulate (h);

σ:Standard deviation around t_{max}(h);

$\alpha(t_{max})$: Maximal probability to sporulate (h^{-1})

Last but not least, the decay rate in the midgut (β) describes the adverse condition inside the vector that leads to a decreasing persistence of our chassis in the midgut, $\beta = \frac{ln(s)}{t_{1/2}}$($t_{1/2}$, bacteria half-life inside the vector). This rate is constant and we selected it for evaluation in experiments with sandflies[2].

Assumptions:

- ➔ Our chassis entry in the germination process only occurs within the midgut;
- ➔ Randomly germination is not considered;
- ➔ Vegetative cells need the same time to form a spore;
- ➔ The sporulation and germination events reach steady-state quickly.

ii) Substrate Flux

$$\frac{d[S]}{dt} = V_{S,intake} - V_{S,rem}$$

Since the lack of information about mathematical models for hematophagous vectors digestion, we decided to reduce the Wolesensky model and results for grasshopper digestion in a simple cosine wave[3]. In our model, this cosine wave function ($S_{intake}(t)$) describes the substrate (i.e. glucose) intake by the sandfly over time. The substrate removal from the midgut system after the blood/sugar meal is a constant rate (R) and the substrate utilization is related to the growth rate ($-\frac{\mu(s)[Bs]}{y}$), both represent the substrate consumption/degradation over time.

$$V_{S,intake} = S_{intake}(t) - \frac{\mu(s)[Bs]}{y} - (R \times S)$$

$$V_{S,rem} \frac{\mu(s)[Bs]}{y} + (R \times S)$$

where,

$$S_{intake}(t) = \frac{S_{in} + S_{in} \times cos(f*t)}{2}$$

$\mu(s)$: *B. subtilis* growth rate (h^{-1});

r: Substrate removal rate (h^{-1});

S_{in}: Substrate per ingestion (µg/L);

y: yield coefficient (dimensionless);

$S_{intake}(t)$: Substrate entry over time (µg/L)

f: Feeding rate (h^{-1});

t: simulation period (h)

$[Bs]$: *B. subtilis* concentration in the midgut (µg/L)

Assumptions:

- ➔ Sandfly's feeding behaviour preserves the same frequency and amplitude over time;
- ➔ Intercompetition in the vector microbiota is disregarded.

II. Antimicrobial Peptide (AMP) Expression Model

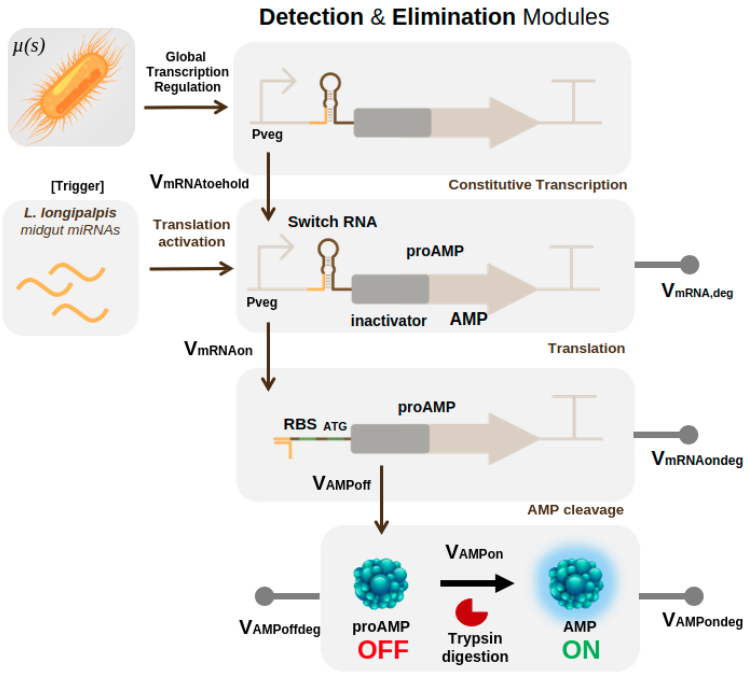

Figure 2: Visual representation of the parameters and functions of circuit

The AMP expression model (Figure 2) is designed to understand the activation of the Detection device and the AMP production levels. By linking the different modeling parts, we

assume that the transcription occurs upon global regulation (growth rate-dependent) (1). The Toehold Switch activation depends on its thermodynamics binding values (2), allowing the AMP production at a constant rate (3). And the trypsin digestion towards AMP activation follows the mass kinetic reactions (4).

i) Transcription

$$[AMP_{DNA}] \rightarrow [AMP_{DNA}] + [mRNA_{toehold}]\ ;\ k_{tx}(\mu(s))$$

For practical purposes, we described a transcription function under global regulation. As the growth rate is measurable under experimental conditions, we considered the growth rate as a proxy for the availability of RNAP. This relationship makes sense since the only growth-dependent parameter is the transcription rate[4,5]. Therefore, the transcription rate will be directly related to the promoter constitutive activity pa_{tx} that has a behaviour described by a Michaelis-Menten rate law.

$$\frac{d[mRNA_{toehold}]}{dt} = V_{tx,toehold} - (V_{mRNA,on} + V_{mRNA,deg})$$

$$V_{tx,toehold} = pa_{tx} . [AMP_{DNA}]$$

$$V_{mRNA,on} = \text{toehold activation (see next section)}$$

$$V_{mRNA,deg} = \phi_{mRNA} . [mRNA_{toehold}]$$

Where,

$$pa_{tx} = V_{max} . \frac{\frac{\mu(s)}{K_m}}{1 + \frac{\mu(s)}{Km}} \sim k_{tx}(\mu(s),)$$

AMP_{DNA}: circuit copy number (unit/cell)

V_{max}: promoter capacity ($nM.min^{-1}$)

Km:promoter activity at half-maximal growth rate (nM)

ϕ_{mRNA}: degradation and dilution rates (min^{-1})

ii) Toehold Activation

$$[mRNA_{toehold}] + [Trigger_{miRNA}] \leftrightarrow [mRNA_{on}]\,;\, k_{on}\,,\, k_{off}$$

Here, we gather our Toehold Design and the kinetic model for evaluating the toehold RNA switch activation upon miRNA trigger presence (as an input), since the toehold thermodynamic values do not represent the system as a whole. However, there is a lack of detailed models for riboswitches, which led us to use the iGEM Athens 2018 model framework to guide this section.

After the translation, our transcripts ($mRNA_{toehold}$) bear a Toehold RNA switch, that blocks ribosome binding and prevents the translation of AMP (OFF state). When the miRNA trigger is present ($Trigger_{miRNA}$), the switch and trigger tend to hybridize, unfolding the hairpin secondary structure, forming an active complex ($mRNA_{on}$) and enabling ribosome binding on the RBS to start the translation (ON state)[6]. This reversible reaction occurs at constant rates, in which k_{on} and k_{off} are the forward and reverse reaction rates for trigger-toehold binding/hybridization, respectively.

$$K_d = \frac{k_{off}}{k_{on}}$$

In this reaction, we assume that the toehold-trigger hybridization is faster than other reactions and quickly reaches the equilibrium state[6,7], an assumption that allows count just bound and unbound states.

$$\frac{d[mRNA_{on}]}{dt} = V_{mRNA,on} - V_{mRNAon,deg}$$

$$V_{mRNA,on} = \frac{[mRNA_{toehold}] \cdot [Trigger_{miRNA}]}{K_d}$$

$$V_{mRNAon,deg} = \phi_{mRNAon} \cdot [mRNA_{on}]$$

$[Trigger_{miRNA}]$: Trigger miRNA concentration available (nM)

V_{max}: promoter capacity (nM.min^{-1})

Km:promoter activity at half-maximal growth rate (nM)

ϕ_{mRNAon}: Trigger-Toehold binding degradation rates (min^{-1})

The first-order equilibrium dissociation constant (K_d) is a thermodynamic parameter that describes the dissociation of a complex between two molecules in solution[8]. In this case, the $[Trigger_{miRNA}]$and $[mRNA_{toehold}]$ pairs with more favorable free energy for the bound state will have lower K_d values[9].

Thermodynamics relations can be exploited to measure the binding affinity and estimate the K_d values. The standard binding Gibbs free energy (ΔG^0), which represents the free energy transaction (from OFF state to ON state) measured under the conditions of 1 atm, T = 298K, and the effective reactant (toehold and trigger) concentrations of 1 M, typically measured in units of kcal/mol, can be related to K_d[8]. In contrast to the Athens 2018 model, assumed an inversely proportional relationship between the estimated ΔG^0 values (from Toehold Design) with K_d.

$$\Delta G^0 = -RTln(\frac{1}{K_d}) \; or \; K_d = -\frac{1}{e^{\Delta G/RT}}$$

R: universal gas constant (cal.K^{-1}.mol^{-1})

T: temperature (K, 298K)

ΔG^0:standard binding Gibbs free energy (kcal/mol)

K_d:equilibrium dissociation constant (nM)

iii) Translation

$$[mRNA_{on}] \rightarrow [AMP_{off}] + [mRNA_{on}]\ ;\ k_{tl}$$

The $[mRNA_{on}]$ starts the translation for $[AMP_{off}]$ production. The translation depends only on the translation rate (k_{tl}), $[mRNA_{on}]$ concentration, $[AMP_{off}]$ activation and degradation rates.

$$\frac{d[AMP_{off}]}{dt} = V_{tl,AMP} - (V_{act,AMP} + V_{AMP,deg})$$

$$V_{tl,AMP} = k_{tl} \,.\, [mRNA_{on}]$$

$$V_{act,AMP} = [AMP_{on}]\ activation\ (see\ next\ section)$$

$$V_{AMP,deg} = \phi_{AMP} \,.\, [AMP_{off}]$$

k_{tl}:translation rate (nM/s)

ϕ_{AMP}: AMP degradation and dilution rates (min^{-1})

iv) AMP activation and dilution

$$[AMP_{off}] + [Trypsin] \rightarrow [AMP_{on}]\ ;\ k_{act}$$

The concentration of [AMPon] is secreted into the midgut and undergoes enzymatic digestion (i.e., trypsinization) for its activation. In reality, the concentration of digestive enzymes in *L. longipalpis* varies according to the blood meal, but for the sake of abstracting this model, we consider enzymatic digestion (activation) at a constant rate (k_{act}). Furthermore, the diffusion of $[AMP_{off}]$to the extracellular medium must be accompanied by a dilution factor (DF) and the total AMP in the medium multiplied by the chassis concentration (cell/L).

$$\frac{d[AMP_{on}]}{dt} = V_{act,AMP} - V_{AMP,deg}$$

$$V_{act,AMP} = k_{act} \frac{[AMP_{off}]}{DF}$$

$$V_{AMP,deg} = \phi_{AMP} . [AMP_{on}]$$

k_{act}:activation rate (nM/s)

DF: dilution factor (-)

ϕ_{AMP}: AMP degradation and dilution rates (min^{-1})

v) Degradation rates

Degradation rates contain half-life of the mRNA and AMP molecules, including a dilution rate represented by the growth rate.

$$V_{mRNA,deg} = \phi_{mRNA} . mRNA_{toehold}$$

$$V_{mRNAon_{deg}} = \frac{ln(2)}{\tau_m} . mRNA_{on}$$

$$V_{AMP,deg} = \phi_{AMP} . AMP$$

Where,

$$\phi_{mRNA} = \frac{ln(2)}{\tau_m} + \mu(s)$$

$$\phi_{AMP} = \frac{ln(2)}{\tau_p} + \mu(s)$$

τ_p: protein/AMP half-life (min)

τ_m:mRNA half-life (min)

$V_{Toeholddeg}$:concentration of $mRNA_{tx/toehold}$ degraded over time (nM/s)

$V_{mRNAdeg}$:concentration of $mRNA_{tx/on}$ degraded over time (nM/s)

V_{AMPoff}:concentration of AMP_{off} degraded over time (nM/s)

Assumptions:

- ➔ Expression leakage not considered. Toehold has high specificity and probability to forming secondary structures resulting in a *leakage rate << translation rate;*
- ➔ The analysis takes place during a constant *L. longipalpis* miRNAs (Trigger) uptake in the intracellular compartment of our *Bacillus subtilis.*
- ➔ We disregard the efficiency of AMP secretion into the extracellular space and the chassis capacity for RNA uptake.

v) Leishmania Death

AMPs have the mechanism of binding by density charge affinity to the cell membrane of the target organism. Their conformational change and/or different aggregation mechanisms increase their toxic activity against the cell. Depending on the characteristic structure of the AMP and the membrane of the target organism, the peptide can undergo a process of aggregation or non-aggregation with low or high cooperativity in a single site or multiple binding sites. Cooperativity occurs when AMP binding can increase affinity by binding other AMPs in the cell membrane, a common event in different studies with this type of peptide[10].

One way to measure the degree of cooperativity is through the Hill Coefficient, which can help to quantify the degree of interaction between membrane-bound AMPs. This coefficient is part of Hill's equation, accompanied by another parameter, the half-saturation constant ($K_{0.5}$), representing the threshold concentration needed for 50% cell death (in the case of AMPs and cells). η determines the sensitivity of response and its value is directly related to the system's response behaviour. Where η> 1 means ultrasensitive response, η<1 represents a sub-sensitive response and η=1 is related to a typical response based on Michaelis Menten.

Therefore, after AMPs production, secretion and activation in the midgut, we evaluated the action of AMP_{on} against *Leishmania spp.*, calculated by the Hill equation as the mortality rate of the parasite. The AMPs selected for our system have high leishmanicidal potential as well as against bacteria, which can harm the growth of our chassis. Finally, the

concentration of *Leishmania spp.* inside the vector was represented by its promastigote (parasite stage) rate of replication (γ) and decay in relation with AMP_{on} concentration.

$$\frac{d[Leish]}{dt} = V_{Leish} - V_{Leishkill}$$

Where,

$$V_{Leishkill} = \frac{AMP_{on}{}^{\eta}}{K_{0.5}{}^{\eta} + AMP_{on}{}^{\eta}}. [Leish]$$

$$V_{Leish} = \gamma. [Leish]$$

γ: Leishmania growth rate (h^{-1});

η:Hill coefficient;

$K_{0.5}$: IC50 for each AMP (nM);

Assumptions:

- ➔ Leishmania grows at a constant rate.

3. SYSTEM OF ODEs

Chassis Growth

$$\frac{d[Bs]}{dt} = V_{Bs,growth} - V_{Bs,death}$$

$$V_{Bs,growth} = \mu(s) \times [Bs]$$

$$V_{Bs,death} = \left(\frac{AMP_{on}^{\ \eta}}{K_{0.5Bs}^{\ \eta} + AMP_{on}^{\ \eta}} + \beta + \alpha(t)\right) \times [Bs]$$

$$\mu(s) = \frac{\mu_{max} \cdot [S]}{Ks + [S]}$$ *(Monod Equation)*

$$\alpha(t_i) = \alpha_{max} \frac{1}{\sqrt{2\pi}\cdot\sigma} exp\left[-0.5\left(\frac{t_i - t_{max}}{\sigma\sqrt{2}}\right)^2\right]$$ (Gaussian function)

Substrate Flux

$$\frac{d[S]}{dt} = V_{S,intake} - V_{S,rem}$$

$$V_{S,intake} = S_{intake}(t) - \frac{\mu(s)[Bs]}{y} - (R \times S)$$

$$V_{S,rem} \frac{\mu(s)[Bs]}{y} + (R \times S)$$

$$S_{intake}(t) = \frac{S_{in} + S_{in} \times cos(f^{*}t)}{2}$$

Transcription

$$\frac{d[mRNA_{toehold}]}{dt} = V_{tx,toehold} - (V_{mRNA,on} + V_{mRNA,deg})$$

$$V_{tx,toehold} = pa_{tx} \cdot [AMP_{DNA}]$$

$$V_{mRNA,deg} = \phi_{mRNA} \cdot [mRNA_{toehold}]$$

$$pa_{tx} = V_{max} \cdot \frac{\frac{\mu(s)}{K_m}}{1 + \frac{\mu(s)}{Km}} \sim k_{tx}(\mu(s),)$$

Toehold Activation

$$\frac{d[mRNA_{on}]}{dt} = V_{mRNA,on} - V_{mRNAon,deg}$$

$$V_{mRNA,on} = \frac{[mRNA_{toehold}] \cdot [Trigger_{miRNA}]}{K_d}$$

$$V_{mRNAon,deg} = \phi_{mRNAon} \cdot [mRNA_{on}]$$

$$K_d = -\frac{1}{e^{\Delta G/RT}}$$

proAMP translation

$$\frac{d[AMP_{off}]}{dt} = V_{tl,AMP} - (V_{act,AMP} + V_{AMP,deg})$$

$$V_{tl,AMP} = k_{tl} \cdot [mRNA_{on}]$$

$$V_{AMP,deg} = \phi_{AMP} \cdot [AMP_{off}]$$

AMP activation

$$\frac{d[AMP_{on}]}{dt} = V_{act,AMP} - V_{AMP,deg}$$

$$V_{act,AMP} = k_{act} \frac{[AMP_{off}]}{DF}$$

$$V_{AMP,deg} = \phi_{AMP} \cdot [AMP_{on}]$$

3.1 PARAMETERS AND INITIAL CONDITIONS

Table 1. Kinetic Model Parameters

Name	Value	Unit	Source	Description	*GSA Notation*
Growth Model					
μ(*s*)	Substrate-dependent	h^{-1}	[11]	*B. subtilis* growth rate.	-
$t_{1/2}$ from β	1.5 (90)	h^{-1} (min^{-1})	[2][a]	single-cell half-life for *B. subtilis* persistence decay rate	*lamb*
α(t)	Time-dependent	h^{-1} (min^{-1})	[1]	B. subtilis sporulation probability rate.	-

[Bs]i	$1x10^2$	cell/L	Estimation from [12][b]	*B. subtilis* inoculation	*Bsi*
μ_{max}	1 (0.016)	h^{-1} (min^{-1})	[11]	Maximal growth rate.	*v*
K_s	0.047	$g.L^{-1}$	[13]	Half-maximal growth rate concentration constant	*Ks*
[S]i	0.3	$g.L^{-1}$	Estimation	Initial Substrate concentration.	*Si*
y	$6.4x10^4$	unit/unit	[14][c]	Yield coefficient	*y*
Rem	0.28 (0.003)	h^{-1} (min^{-1})	Estimation	Substrate removal rate	*R*
S_{in}	0.03	$g.L^{-1}$	Estimation	Substrate concentration per blood/sugar feeding	-
f	0.01 (0.0016)	h^{-1} (min^{-1})	Estimation	Feeding frequency	*freq*
α_{max}	0.13	-	[1]	Maximal proportion of sporulating vegetative cells	*alphamax*
t_{max}	74.4 (4464)	h (min)	[1]	Time at maximal probability to sporulate	*tmax*
σ	12 (720)	h (min)	[1]	Standard deviation around tmax	*sig*
$K_{0.5Bs}$	2 x $K_{0.5\ Leish}$	nM	See Leishmania Death parameters	IC50 of AMPs against *B. subtilis*	*K05Bs*
AMP Expression Model					
AMP_{DNA}	1	unit/cell	Genome integration	Circuit copy number	*DNA*
$\mu(s)$	-	min^{-1}	See Growth Model	B. subtilis growth rate.	-
$V_{max_{tx}}$	50	$nM.min^{-1}$	Estimation from UNESP 2018 team	Maximal promoter activity	*Vmaxtx*
Km_{tx}	0.013	min^{-1}	[5]	Growth rate at half-maximal promoter activity	*Km*
ktl	150	min^{-1}	Estimation from Freiburg 2016 team	Translation rate	*ktl*
R	1985	$cal.K^{-1}.mol^{-1}$	-	Universal gas constant	*gas*
T	310	K	-	Temperature	*T*
ΔG^0	- (~-30)	kcal/mol	From Toehold Switch Design	Standard binding Gibbs free energy	*DeltaG0*
$[Trigger]$	100	nM	Estimation	Initial Trigger concentration	*Trigger*

k_{act}	0.8	min^{-1}	Estimation	AMP activation rate in the midgut	*dig_rat*
FD	10000	-	Estimation	Dilution factor for midgut	*FD*
Leishmania Death					
γ	0.0016	min^{-1}	Estimation	Leishmania growth rate	*growthLeish*
η	2	-	Estimation	Hill Coefficient	*n*
$D1K_{0.5}$	8100	nM	[15]	IC50 of DRS-N1 against *L. infantum*	*K05*
$D2K_{0.5}$	15000	nM	[16]	IC50 of DRS-H3 against *L. infantum*	*K05*
$D3K_{0.5}$	4700	nM	[17]	IC50 of DRS-S1 against *L. infantum*	*K05*
$CWK_{0.5}$	7000	nM	Estimation	IC50 of CAM-W against *L. infantum*	*K05*
$[Leish]_i$	$3x10^3$	cell/L	[18]	Initial Leishmania concentration within the vector.	*Leish1*
Degradation					
$\tau\, m$	3	min	[19]	mRNA half-life	*Tm*
$\tau\, p$	4.2	min	[19]	Protein/AMP half-life	*Tp*
Initial Conditions					
[Bs]i	10^2	cell/L	Estimation from [12]	Digestion of *initial B. subtilis* concentration	*Bsi*
[S]i	0.03	$g.L^{-1}$	Estimation	Initial Substrate concentration[d]	*Si*
$[Trigger]$	10	nM	Estimation	Initial Trigger concentration	*Trigger*
$[Leish]_i$	$3x10^3$	cell/L	[18]	Initial Leishmania concentration inside the vector.	*Leish1*

a) Mean values of B. subtilis persistence within 24h in *L. longipalpis larvae* gut;
b) 10^2 Cells/L = 10^5 CFU/mL from [12]
c) Bacteria unit per substrate concentration (rescaled)
d) This value remains for each substrate uptake over time (See Substrate Flux).

References

[1] Gauvry, E. et al. (2019) Differentiation of Vegetative Cells into Spores: a Kinetic Model Applied to Bacillus subtilis. Applied and Environmental Microbiology, 85(10). Article
[2] Heerman, M. et al. (2015) Bacterial Infection and Immune Responses in Lutzomyia longipalpis Sand Fly Larvae Midgut. PLOS Neglected Tropical Diseases, 9(7). Article
[3]Wolesensky, W. et al. (2005) A model of digestion modulation in grasshoppers. Ecological Modelling, 188(2-4), p. 358-373. Article
[4] Nordholt, N. et al. (2017) Effects of growth rate and promoter activity on single-cell protein expression. Nature Scientific Reports, 7(6299). Article
[5] Gerosa, L. et al. (2013) Dissecting specific and global transcriptional regulation of bacterial gene expression. Molecular Systems biology, 9(658). Article
[6] Senoussi, A. et al. (2011) Quantitative characterization of translational riboregulator using an in vitro transcription-translation system. ACS Synthetic Biology, 7(5), p. 1269-1278. Article
[7] Hong, F. et al. (2020) Precise and Programmable Detection of Mutations Using Ultraspecific Riboregulators. Cell, 180(5), p. 1018-1032. Article
[8] Thevendran, R. et al. (2020) Mathematical approaches in estimating aptamer-target binding affinity. Analytical Biochemistry, vol. 600. Article
[9] Alon, U. (2019) An Introduction to Systems Biology: Design Principles of Biological Circuits. Second Ed., Taylor & Francis, Appendix B. Book
[10] Srinivasan, S. et al. (2020) A steady-state modeling approach for simulation of antimicrobial peptide-membrane interaction. BBA-Biomembranes, 1862(4). Article
[11] Ugalde-Salas, P. et al. (2020) Insights from Microbial Transition State Theory on Monod's Affinity Constant. Nature Scientific Reports, 10(5323). Article
[12] Wang, S. et al. (2017) Driving mosquito refractoriness to Plasmodium falciparum with engineered symbiotic bacteria. Science, 357(6358), p. 1399-1402. Article
[13] Wang, X. et al. (2015) Modeling of the Bacillus subtilis Bacterial Biofilm Growing on an Agar Substrate. Hindawi: Computational and Mathematical Methods in Medicine, vol. 2015. Article
[14] Overkamp, W. et al. (2014) Physiological and cell morphology adaptation of Bacillus subtilis at near-zero specific growth rates: a transcriptome analysis. Environmental Microbiology, 17(2). Article
[15] Brand, G. D. et al. (2013) The Skin Secretion of the Amphibian Phyllomedusa nordestina: A source of Antimicrobial and Antiprotozoal Peptides. Molecules, 18(6), 7058-7070. Article
[16] Brand, G. D. et al. (2006) Novel dermaseptins from Phyllomedusa hypochondialis (Amphibia). Biochemical and Biophysical Research Communications, 347(3). Article
[17] Pérez-Cordero, J.J. et al. (2011) Leishmanicidal activity of synthetic antimicrobial peptides in an infection model with human dendritic cells. Peptides, 32(4), p. 683-690. Article
[18] Serafim, T. D. et al. (2018) Sequential blood meals promote Leishmania replication and reverse metacyclogenesis augmenting vector infectivity. Nature Microbiology, vol. 3, p. 548-555. Article
[19] Radeck, J. et al. (2013) The Bacillus Biobrick Box: generation and evaluation of essential genetic building blocks for standardized work with Bacillus subtilis. Journal of Biological Engineering. 7(29). Article

Biopank is sponsored by